

Chondroprotective effects of platelet lysate towards monoiodoacetate-induced arthritis by suppression of TNF- α -induced activation of NF- κ B pathway in chondrocytes

Li Yan^{1,2,*}, Li Zhou^{1,2,*}, Danting Xie², Wenxi Du¹, Fangming Chen³, Qiang Yuan⁴, Peijian Tong¹, Letian Shan^{1,2}, Thomas Efferth⁵

¹The First Affiliated Hospital, Zhejiang Chinese Medical University, Hangzhou, China

²Center for Stem Cell Translational Research, Zhejiang Chinese Medical University, Hangzhou, China

³Academy of Chinese Medical Sciences, Zhejiang Chinese Medical University, Hangzhou, China

⁴College of Pharmacy, Zhejiang Chinese Medical University, Hangzhou, China

⁵Department of Pharmaceutical Biology, Institute of Pharmacy and Biochemistry, Johannes Gutenberg University, Mainz, Germany

*Equal contribution

Correspondence to: Wenxi Du, Peijian Tong, Letian Shan; **email:** purpleraineer@163.com, tongpeijian@163.com, letian.shan@zcmu.edu.cn

Keywords: platelet lysate, growth factor, osteoarthritis, TNF- α , NF- κ B

Received: December 15, 2018

Accepted: May 2, 2019

Published: May 14, 2019

Copyright: Yan et al. This is an open-access article distributed under the terms of the Creative Commons Attribution License (CC BY 3.0), which permits unrestricted use, distribution, and reproduction in any medium, provided the original author and source are credited.

ABSTRACT

Platelet lysate (PL) contains a cocktail of growth factors that actively participates in cartilage repair. This study was designed to determine the effect and mechanism of PL on osteoarthritis (OA). An arthritis model was established to mimic human OA by intra-articular injection of monoiodoacetate (MIA) to Sprague Dawley (SD) rats. The model was weekly treated with PL by intra-articular injection. Thermal withdrawal latency, mechanical withdrawal threshold, and treadmill gait were tested for pain behavior observation. Histopathological and immunohistochemical analyses were conducted for evaluating cartilage degradation. Real time PCRs and Western blots were conducted to elucidate the mechanism of PL on primary chondrocytes. Results showed that, *in vivo*, PL significantly attenuated pain symptoms and exerted chondrocyte-protective and extracellular matrix (ECM)-modifying effect on the arthritic cartilage in a dose-dependent manner. The *in situ* expressions of type II Collagen (Col2) and matrix metalloproteinase 13 (Mmp13) in the arthritic cartilage was abnormal and was restored by PL. *In vitro*, PL significantly restored tumor necrosis factor α (TNF- α)-suppressed anabolic gene expression (Col2 and aggrecan) and TNF- α -increased catabolic gene expression (Col10, Mmp13, Adamts5, and Adamts9) in chondrocytes. The effects were mediated by TNF- α downstream signaling, including inhibition of NF- κ B and c-Jun activities. This study provides certain knowledge of anti-OA effect and TNF signaling-related mechanism of PL, placing it as a promising and alternative option for OA therapy in the future.

INTRODUCTION

Osteoarthritis (OA) of the knee is the most common joint disease characterized by progressive destruction of articular cartilage, thinning and eventual wearing of

cartilage, thus resulting in joint pain and limited joint movement [1]. The pain and joint dysfunction of OA place a major burden on communities as well as health and social care systems, making OA a leading cause of global disability [2]. It is estimated that 15% of the

world populations suffer from OA, including more than 39 million Europeans and more than 20 million Americans [3]. By 2020, these numbers will probably be doubled [4]. Due to the limitation of intrinsic self-repairing capacity of the load-bearing articular cartilage of joint, even minor lesions or injuries may lead to progressive damage, joint degeneration, and finally OA [1]. Many therapeutic efforts have been made for OA treatment. Surgical approaches, such as knee arthroplasty, are successfully used for addressing end-stage OA. However, adverse outcomes have some possibility to occur with the surgeries, including high cost and limited lifespan of prostheses. Preoperative non-surgical approaches, such as intra-articular pharmacological injections, are more important for the treatment of early- and middle-stage OA. This includes both intra-articular corticosteroid and visco-supplementation injections, which seemingly have successful, albeit short-term benefits to OA patients, including pain relief and knee function improvement [5, 6]. However, the clinical practice guidelines of the American Academy of Orthopaedic Surgeons demonstrated inconclusive evidence to recommend for or against corticosteroid and strong evidence against hyaluronic acid (HA) visco-supplementation injections for OA patients [7]. This has led to the emergence of other injectable options for symptom relief and functional improvement in these patients [8].

In the 1980s, human platelet lysate (PL) prepared by repeated freeze/thaw cycles from peripheral blood or platelet concentrates were firstly described to support proliferation of primary and established cell lines and to promote tissue regeneration and wound healing [9, 10]. PLs have a strong growth promoting action on primary articular chondrocytes, which promote growth and sulfated glycosaminoglycan synthesis of articular chondrocytes [11]. The bioactivity of PL was derived from a series of potent bioactive mediators primarily in α -granules of platelet [12]. A variety of growth factors account for these effects, such as platelet derived growth factors (PDGF), transforming growth factor- β (TGF- β), insulin-like growth factor (IGF-1), epidermal growth factor (EGF), and vascular endothelial growth factor (VEGF) [13, 14]. Those anabolic growth factors stimulate chondrocyte synthesis of proteoglycans, aggrecan and type II collagen, induce chondrocyte proliferation, trigger chondrogenic differentiation of mesenchymal stromal cells, and decrease the catabolic effects of cytokines such as interleukin-1 (IL-1) and the matrix metalloproteinases (MMP) [15]. For example, PDGF and IGF-1 are potent inhibitors of IL-1 β -mediated apoptosis of chondrocytes in OA [16], and PDGF, TGF- β , IGF-1 and EGF are regulators of cartilage growth, which can improve chondrocyte metabolism

[17, 18]. Recently, intra-articularly injected autologous PL has been reported as an efficient method for temporarily managing OA of the distal interphalangeal joint in athletic horses [19]. In addition, intra-articular autologous PL significantly improved the non-normalized Knee Osteoarthritis and Disability Outcome Score (KOOS) of patients with early and intermediate knee OA in an open-label prospective study [20]. This is certainly a clue that PLs containing growth factors have a promising potential for treatment of OA.

To confirm the therapeutic effect and mechanism of PL on OA, we established an animal model of arthritis by intra-articular monoiodoacetate (MIA)-injection and a cellular model of arthritic chondrocytes by TNF- α treatment. MIA induces cartilage degeneration through production of pro-inflammatory cytokines, damage of pain-related sensory innervation of dorsal root ganglia, induction of cell death, disruption of chondrocyte metabolism and decrease of proteoglycan content, which causes rapidly progressing OA with less invasive procedures and enables standardization [21, 22]. The MIA model is commonly used as an arthritis model mimicking human OA for pain assessment, owing to the consistent pain-like responses throughout the modeling period [23]. It provides measurable changes on joint movements, tactile allodynia, inflammation, and progressive cartilage degeneration that represent markers for OA evaluation [24]. Previous studies reported that the MIA model is useful for evaluating the pathology of non-traumatic OA, pain mechanisms, and therapeutic effects on cartilage [25, 26]. Therefore, this model has been recommended as preferred model to study chondroprotective and analgesic agents compared to the existing surgical and spontaneously developing models [27]. Articular cartilage is a conjunctive tissue composed of only one cell type, chondrocytes, enclosed in a self-synthesized extracellular matrix (ECM) [28]. These specific cells represent approximately 1% of the total cartilage volume and are responsible for matrix composition and integrity. Thereby, they confer to mechanical support and joint lubrication of cartilage [28, 29]. During OA development, pro-inflammatory cytokines, such as TNF- α , participate in cartilage degradation through activation of chondrocyte catabolism. Elevated concentrations of TNF- α in synovial fluid have also been demonstrated in patients with knee OA disease progression [30]. Therefore, we applied TNF- α -treated chondrocytes as OA-like *in vitro* model and performed cellular and molecular experiments to evaluate the therapeutic mechanism of PL. To the best of our knowledge, this is the first time to report on the anti-OA mechanism of PL.

RESULTS

Quality control of PL

CD61 is a specific cell surface marker for rat platelet. Flow cytometry analysis for CD61 surface marker expression revealed positive populations of platelet in platelet concentrates prior to PL preparation. As shown in Figure 1, the platelet concentrates contained $93.4 \pm 2.7\%$ of CD61-positive cells with CD61-positive rate of $93.9 \pm 2.9\%$. After freeze-thaw lysis, PL was obtained and found containing $17.0 \pm 2.3 \mu\text{g/ml}$ of PDGF, $96.9 \pm 4.0 \mu\text{g/ml}$ of IGF-1, $18.0 \pm 4.0 \mu\text{g/ml}$ of TGF- β , $1.0 \pm 0.2 \mu\text{g/ml}$ of EGF, and $0.4 \pm 0.04 \mu\text{g/ml}$ of VEGF.

Anti-nociceptive effect of PL

OA-induced knee pain response and anti-nociceptive effect of PL were shown in Figure 2. MWT reflected mechanical allodynia and TWL reflected thermal hyperalgesia. Spontaneous activity and gait parameters (total paw area and unit stride length) reflected pain-

related behaviors. On the day 28, levels of all the parameters in the model group were significantly decreased, when compared with that of the normal group (all $P < 0.01$), indicating typical knee pain responding to arthritis modeling. When compared with the model levels, PL significantly restored the levels of above parameters toward normal levels after 28-day treatment (all $P < 0.01$).

Therapeutic effect of PL on arthritic rats

Results of histopathological staining were illustrated in Figure 3. Cartilage degeneration, exhibited by apoptosis of chondrocytes, loss of collagen mass, disorganization of matrix, and irregularity of cartilage surface, was seen in the arthritis model group with significantly increased Mankin's score and OARSI score (both $P < 0.01$ versus NC). In the PL-treated groups, the degeneration was gradually reversed by PL in a dose-dependent manner, with significantly decreased Mankin's score and OARSI score ($P < 0.05$ or $P < 0.01$ versus model). It can be observed that the number of chondrocytes, mass of collagen in matrix, and cartilage surface were remarkably improved by increasing doses of PL.

Results of immunohistochemical analysis were shown in Figure 4. The NC group showed normal expression of Col2 in cartilage, whereas the arthritis group expressed an obvious loss of Col2 in cartilage with significant smaller positive area ($P < 0.01$ versus NC). The Col2 expression was obviously upregulated and its positive area significantly increased by PL in a dose-dependent manner (all $P < 0.01$ versus model), and it even reached a normal-like phenotype with PL-H treatment. Moreover, the cartilage in NC group showed almost negative Mmp13 immunoreactivity, whereas that in the arthritis model expressed stronger Mmp13 immunoreactivity with larger positive area ($P < 0.01$ versus NC). The Mmp13 immunoreactivity was remarkably decreased and its positive area significantly shrank by PL treatment in a dose-dependent manner (all $P < 0.01$ versus model). It can be seen that both PL-M- and PL-H-treated cartilage were almost restored to the normal phenotype.

Cellular and molecular effects of PL on chondrocytes

As shown in Figure 5 (upper left), PL derived from a dose range of 10^3 to 10^8 platelets significantly increased the chondrocyte viability with increasing proliferative rate from $0.05 \pm 9.81\%$ to $30.74 \pm 13.15\%$ at 24 h and from $3.37 \pm 4.69\%$ to $46.14 \pm 10.6\%$ at 48 h. Thus, the proliferative effect of PL on chondrocytes was dose-dependent. The regulative effects of PL on gene expressions of chondrocytes were analyzed using qPCR assay. For mimicking OA condition, chondrocytes were pretreated with TNF- α . As shown in Figure 5 (upper right and lower), TNF- α significantly downregulated the

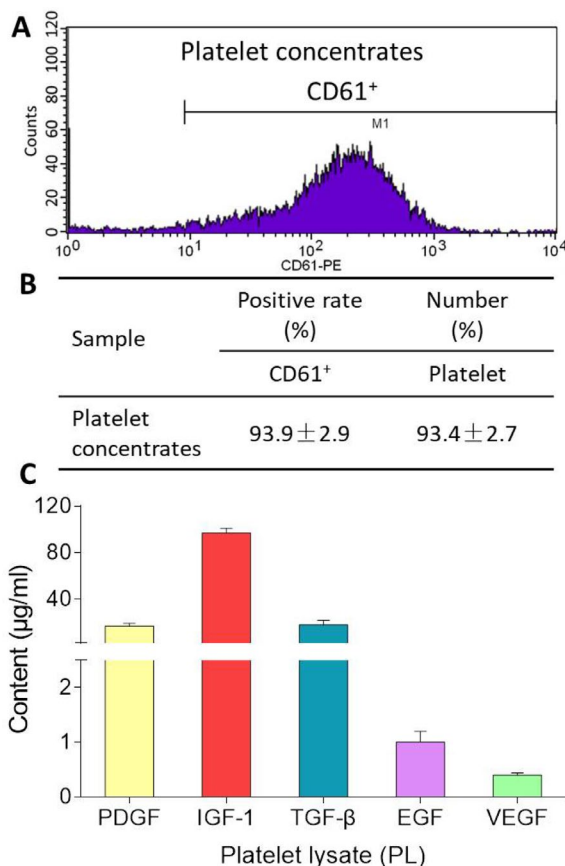


Figure 1. Flow cytometry pattern of platelet concentrates (A), CD61-positive rate and platelet number of platelet concentrates (B), and contents of PDGF, IGF-1, TGF- β , EGF, VEGF in PL (C). Values are presented as mean \pm SD, $n = 3$.

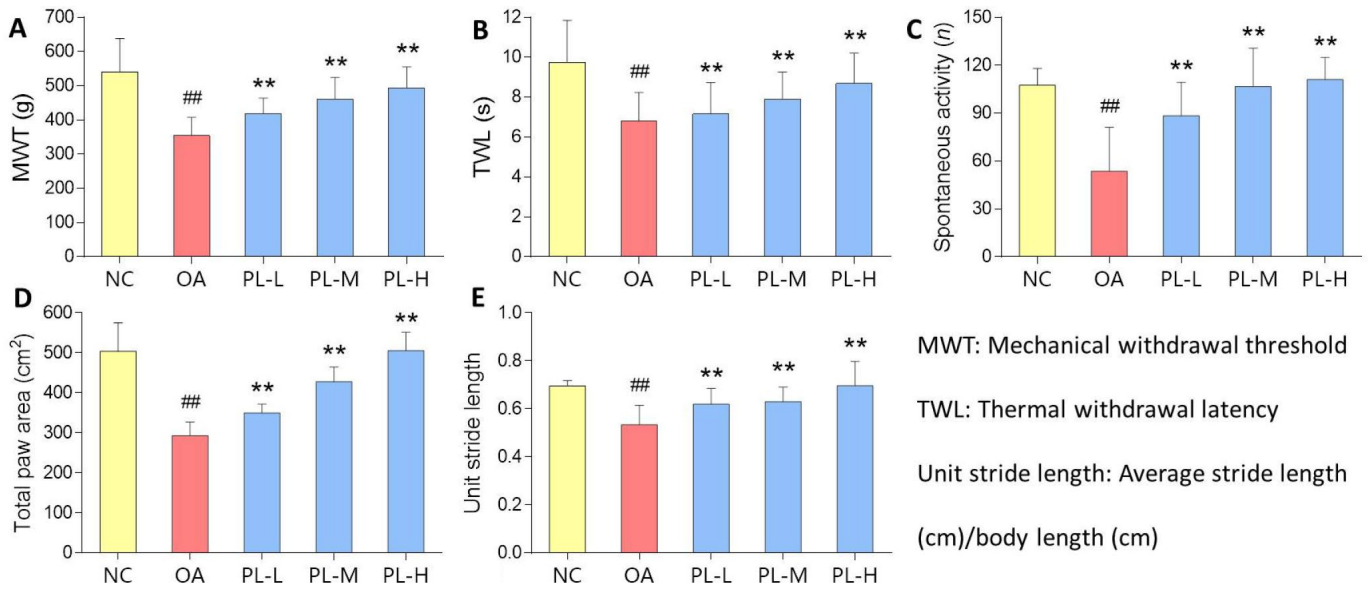


Figure 2. Pain-related behavioral results of rats with PL treatment for 4 weeks. (A) MWT (g); (B) TWL (s); (C) Spontaneous activity (n); (D) Total paw area (cm²); (E) Unit stride length. Values are shown as mean ± SD. ^{##}*P* < 0.01 vs. NC group; ^{**}*P* < 0.01 vs. model group.

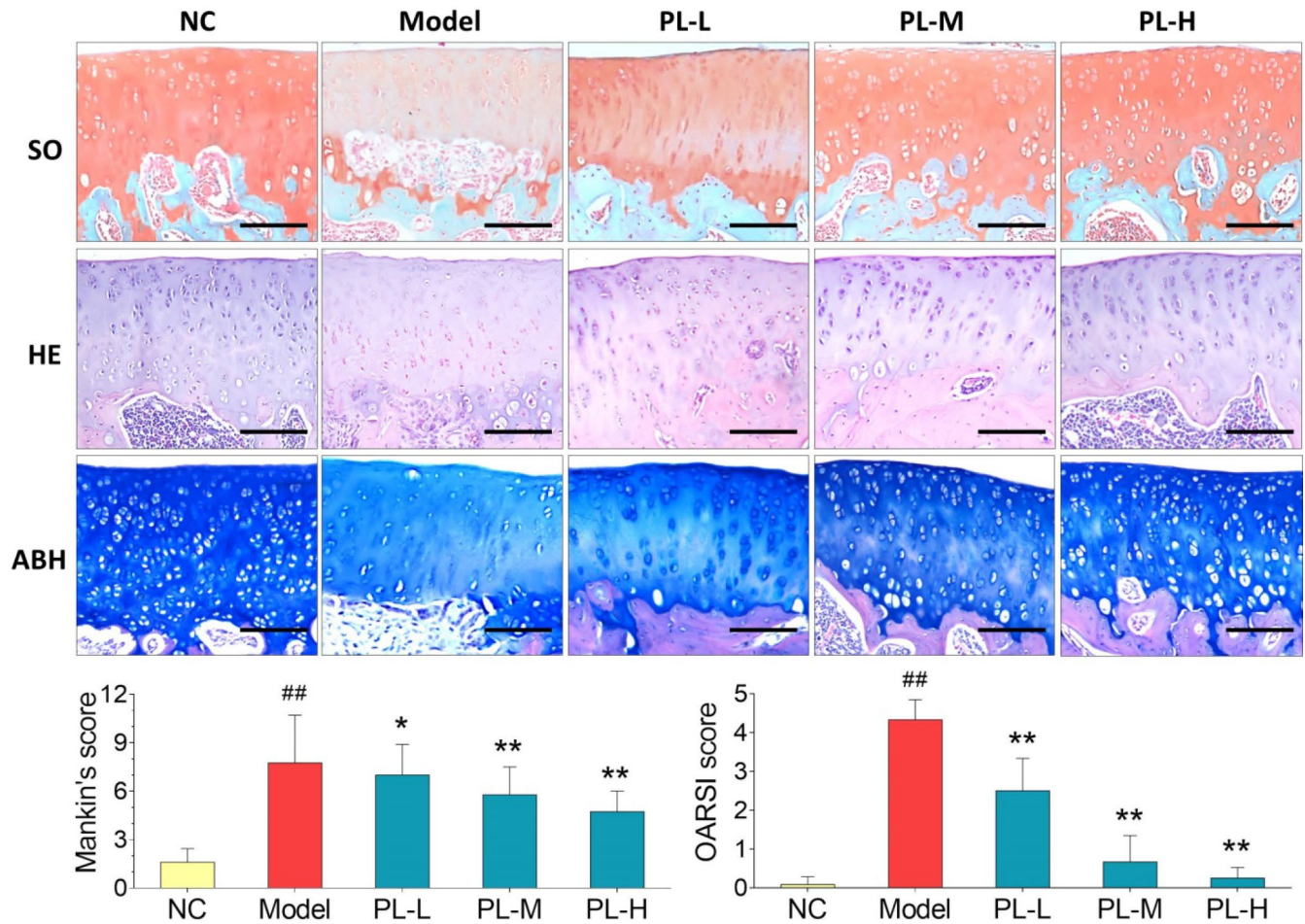


Figure 3. Observation of histopathological stainings (HE, SO, and ABH) with Mankin's scoring and OARSI scoring of rat joints. Values are shown as mean ± SD. ^{##}*P* < 0.01 vs. NC group; ^{*}*P* < 0.05 or ^{**}*P* < 0.01 vs. model group. Scale bar = 100 μm.

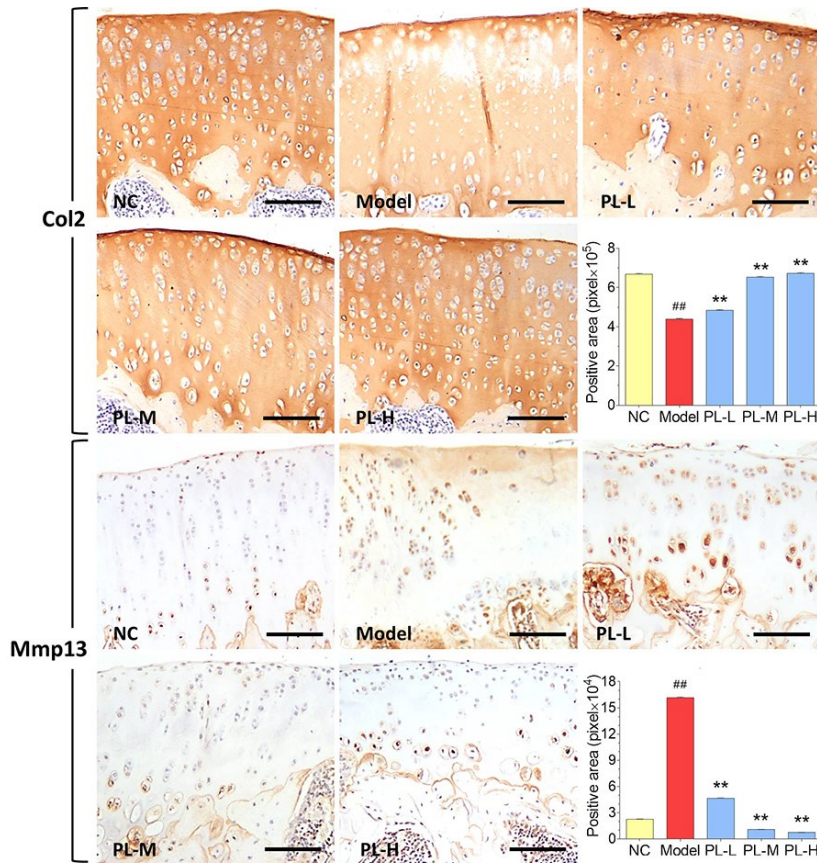


Figure 4. Immunohistochemical observation and semiquantified positive area of Col2 and Mmp13 expressions in rat cartilage. Scale bar = 100 μ m.

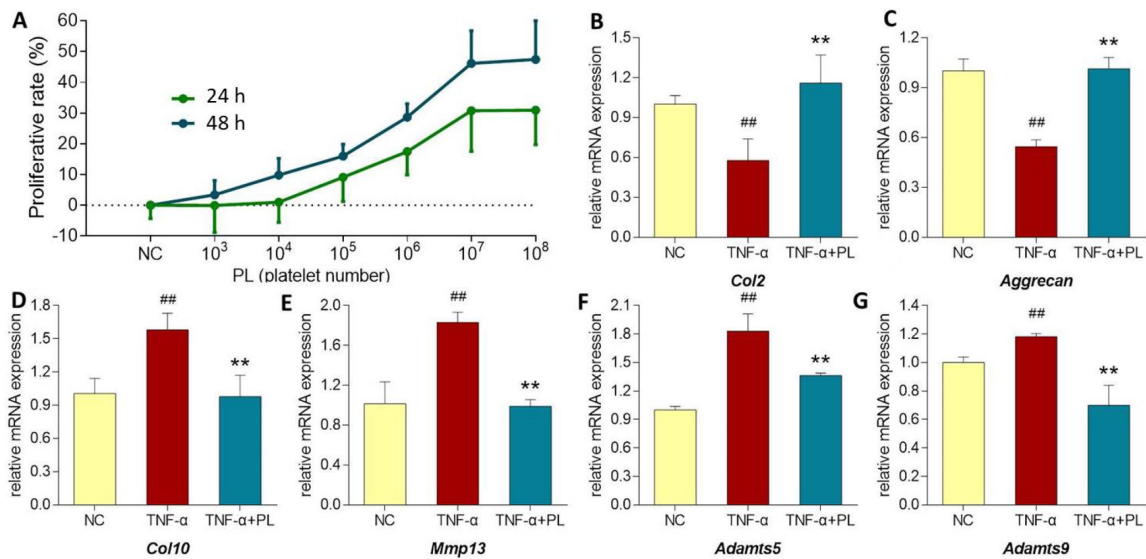


Figure 5. (A) Chondrocyte viability at 24 h and 48 h after PL treatment. (B–G) Relative mRNA expressions of target genes in chondrocytes treated with only TNF- α or TNF- α plus PL. (B) Col2 expression; (C) Aggreacan expression; (D) Col10 expression; (E) Mmp13 expression; (F) Adamts5 expression; (G) Adamts9 expression. Values are shown as mean \pm SD. ## P < 0.01 vs. normal cells; * P < 0.05 or ** P < 0.01 vs. TNF- α treated cells.

expressions of *Col2* and *aggrecan* and upregulated the expressions of *Col10*, *Mmp13*, *Adams5*, and *Adams9*, as compared with that of NC group (all $P < 0.01$). The altered expressions of those genes were significantly reversed by PL after 24 h treatment, as compared with that of TNF- α group ($P < 0.05$ or $P < 0.01$).

TNF signaling pathway-related mechanism of PL

As shown in Figure 6, TNF- α significantly activated the phosphorylation of NF- κ B p65, IKK α/β , and c-Jun (all $P < 0.01$ versus normal levels), and upregulated the protein expressions of Col10, PARP, c-PARP, and Mmp13, (all $P < 0.01$ versus normal levels). In comparison, PL significantly inhibited the phosphorylation of NF- κ B p65, IKK α/β , and c-Jun (all $P < 0.01$) and downregulated the expressions of Col10, PARP,

c-PARP, and Mmp13 (all $P < 0.01$) toward the normal levels.

DISCUSSION

Aging is an important contributing factor to the development of OA, the mechanisms of which appear to be multi-factorial and may include age-related pro-inflammatory state termed “inflamm-aging” [31]. Higher levels of pro-inflammatory cytokines, such as TNF- α and IL-1 β , have been shown to correlate with pain and physical function in older adults with knee OA [32]. The components of joint tissues, including the cartilage and meniscus, can be a source of pro-inflammatory mediators, in which an increased expression of pro-inflammatory cytokines was found in chondrocytes from older tissue donors with OA [33].

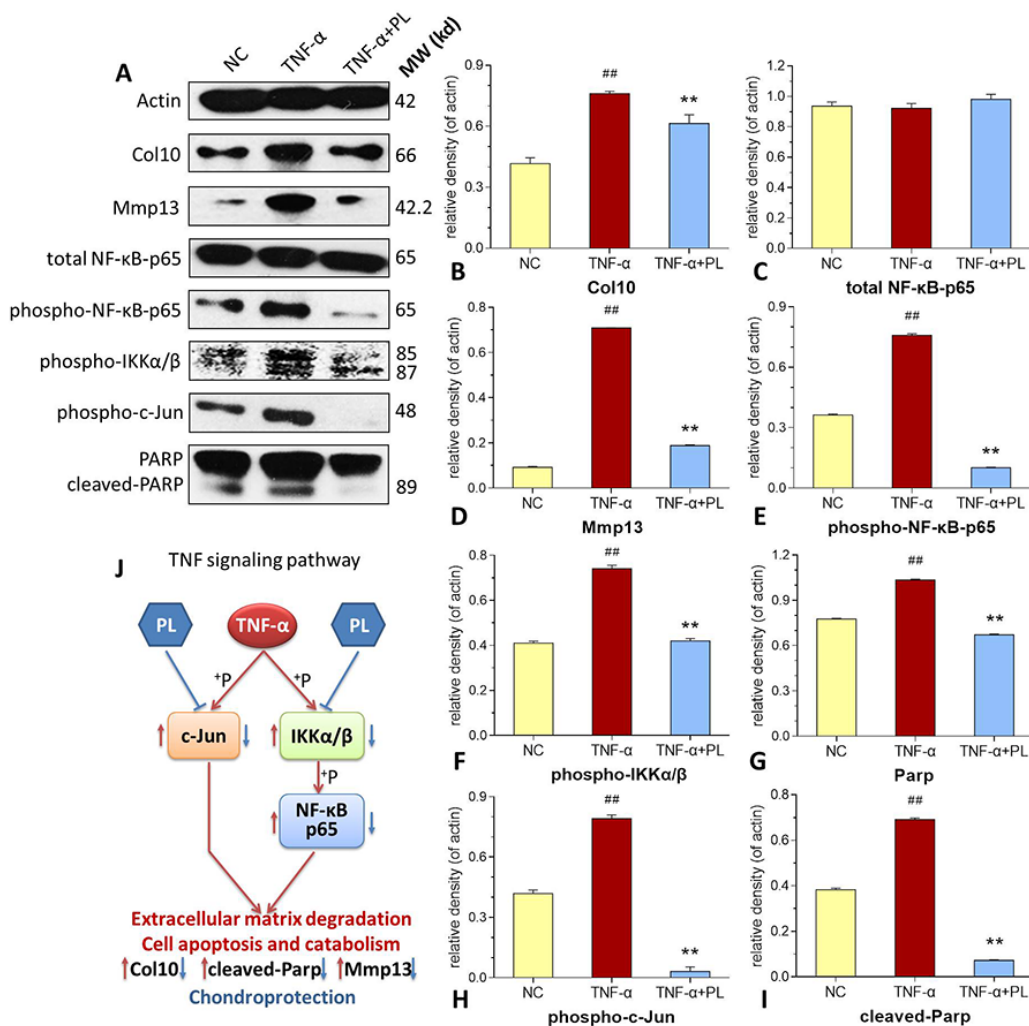


Figure 6. (A–I) Expression and phosphorylation of target proteins in chondrocytes. (A) electrophoretic profile; (B) Col10 expression; (C) total NF- κ B-p65 expression; (D) Mmp13 expression; (E) phospho-NF- κ B-p65 expression; (F) phosphor-IKK α/β expression; (G) PARP expression; (H) phosphor-c-Jun expression; (I) cleaved-PARP expression. (J) deduced process of relative TNF signaling pathway. Values are shown as mean \pm SD. $##P < 0.01$ vs. normal cells; $*P < 0.05$ or $**P < 0.01$ vs. TNF- α treated cells.

Breakdown of those components are handled by a set of aggrecanases (*e.g.*, a disintegrin and metalloproteinase with thrombospondin motifs, Adams) and collagenases (matrix metalloproteinases, Mmps), which are upregulated by pro-inflammatory cytokines through activation of pathways such as NF- κ B in early and late OA [28, 34, 35]. These proteases are key catabolic regulators of cartilage destruction, making anti-catabolic therapy, especially that which targets pro-inflammatory cytokine-associated pathways, an attractive strategy to counteract OA. Growth factors, such as IGF-1 and PDGF, reversed the cartilage inflammation and catabolic actions by suppressing pro-inflammatory cytokine-induced transcription of the genes involved in inflammation, cartilage degradation, and chondrocyte apoptosis [16]. Therefore, growth factors may provide PL great potential in treating pro-inflammatory cytokine-associated OA.

In this study, PL was derived from concentrated platelets with high purity of >93% and contained growth factors including IGF-1, PDGF, and TGF- β (Figure 1). The data of animal experiment showed a strong anti-nociceptive effect of PL that dose-dependently reversed the MIA-induced mechanical allodynia, thermal hyperalgesia, reduced spontaneous activity, and abnormal gait patterns (Figure 2). A dose-dependent chondrocyte-protective and ECM-modifying effect was also found exerted by PL on the MIA-induced cartilage degradation (Figures 3 and 4). *In vitro*, PL upregulated the TNF- α -suppressed anabolic molecules (*Col2* and *aggrecan*) and downregulated the TNF- α -activated catabolic molecules (*Col10*, *Mmp13*, *Adamts5*, and *Adamts9*) (Figures 5 and 6). *Col2* and *aggrecan* are the main components of cartilage, which give cartilage tensile strength and resistance to load-bearing compression [36]. Collagenase- and aggrecanase-induced degradation of *Col2* and *aggrecan* is an early pathological marker of OA. *Mmp13* acts as the major collagenase while *Adamts5/9* as major aggrecanase, degrading *Col2* and *aggrecan* in cartilage during OA progression [37, 38]. Gene deletion of the *Mmp13* or *Adamts 5* decelerated OA progression by inhibiting cartilage degeneration after surgical OA modeling [39, 40]. *Col10* is a late-stage chondrocyte hypertrophy marker upregulated in OA cartilage as a result of chondrocyte hypertrophy and cartilage calcification [41]. It is associated with cartilage degradation and inflammation in patients with various degrees of OA [42]. Expressions of the above anabolic and catabolic molecules were abnormally altered by TNF- α and restored by PL, indicating that TNF signaling mediated mechanisms may have contributed to PL's effect.

The TNF- α activated NF- κ B pathway plays an important role in TNF signaling during OA cartilage destruction [43]. In this pathway, phosphorylation of IKK α/β and NF- κ B p65 (p65) mediates the regulation of promoter activity of both anabolic and catabolic genes in chondrocytes. For example, phospho-p65 translocated from the cytoplasm to the nucleus, strongly activating the human *ADAMTS5* and *MMP13* activities [44, 45]. The knockdown of p65 with specific siRNA inhibited the expression of cartilage catabolic factors in chondrocytes [46]. In this study, phosphorylation of both IKK α/β and p65 were activated by TNF- α , but inhibited by PL (Figure 6). This suggests that PL rebalanced chondrocyte anabolism-catabolism through the TNF/NF- κ B pathway. Moreover, our data showed that the phosphorylation of c-Jun in chondrocytes was enhanced by TNF- α , but markedly blocked by PL (Figure 6). c-Jun is a crucial downstream molecule in another TNF signaling pathway, the TNF/JNK pathway [47]. JNKs (c-Jun N-terminal kinases) are involved in chondrocyte proliferation and apoptosis as well as catabolism [48, 49]. Activated JNK phosphorylates its nuclear substrate, c-Jun, a transcription factor for the activator protein 1 (AP-1), mediating catabolic transcription and cell apoptosis/death [47, 50]. Thus, a blockage of phosphorylation on JNK or c-Jun prevents chondrocyte degradation and apoptosis/death in OA [51]. In this study, PL induced chondrocyte proliferation and blocked the phosphorylation of c-Jun and cleavage of PARP in chondrocytes (Figures 5 and 6), implying that, except for the TNF/NF- κ B pathway, TNF/JNK pathway might also mediate the chondroprotective mechanism of PL. Further studies are warranted to elucidate more details of the TNF/JNK pathway mediated molecular mechanisms of PL.

Autologous platelet rich plasma (PRP) is a famous and popular non-operative treatment modality for tissue repair, especially for repairing cartilage injuries [52]. The efficacy of PRP is largely dependent on its functional components, a concentrated cocktail of growth factors stored in platelets. Findings from current studies suggest that PRP is a promising treatment for repairing cartilage defects, attenuating OA symptoms and improving joint function with an acceptable safety profile [53]. However, the efficacy of PRP for clinical applications remains unpredictable and controversial, owing to the lack of appropriate controls for validation and variable outcome data [54]. The drawbacks of PRP includes: (1) not all growth factors are released from PRP without extrinsic activation, and the heterologous activators, such as thrombin and CaCl₂, may cause unpredictable adverse events; (2) the presence of fibrinogen and the formation of fibrin clots after thrombin stimulation may trap partial growth factors, resulting in the loss of bioactive factors; (3) highly

variable methods for preparation and activation of PRP and high individual differences between different donors results in variable platelet number and growth factor content, especially when no standardized preparation and quality control was available for PRP; and (4) the storage temperature of PRP should be no less than 4 °C and the storage period is short, suggesting an immediate use after the preparation [55, 56]. PL is the next generation product of PRP, which overcomes these drawbacks by replacing PRP. It reveals the following advantages: (1) The freeze-thaw cycle is a mechanical method for activation of platelets, which avoids the use of heterologous activators and their unnecessary interference; (2) cellular debris and WBC contamination are removed during PL preparation, which remain in PRP; (3) PL contains higher contents of growth factors than that of PRP, owing to the freeze-thawing disruption of a mass of platelets; (4) it is much easier to standardize the product of PL by analyzing the growth factor content before its use, and the content is nearly independent from different donors; and (5) PL can be stored frozen for a long time, resulting in a long term use for consecutive applications [55, 56]. Without doubt, PL exerts stronger and more consistent effects compared to standard PRP's [56]. A previous study on commercially obtained PL has reported that PL was effective in supporting monolayer expansion of FBS-free chondrocytes and proliferation of FBS-free chondrocytes in chondrogenic pellet culture [51]. Although the commercial PL led to rapid proliferation, the PL-expanded chondrocytes showed lower productions of sGAG and total collagen as well as lower gene expressions of *COL2* and *ACAN* than FBS-expanded chondrocytes, from which the authors concluded that PL might not be ideal for cell therapies [57]. However, these results were opposite to other findings that PL-expanded chondrocytes produced more sGAG than FBS-expanded chondrocytes in micromass pellets [58]. Such contradiction could be due to the difference in their preparation techniques. Clearly, more work needs to be done to standardize the preparation procedure for optimal therapeutic outcome. In this study, our results showed chondroprotective effect of PL on chondrocytes, which might be steady and replicable owing to the quality control on cytokine profile we made.

Taken together, the overall results demonstrated that PL effectively ameliorated pain symptoms and prevented cartilage degradation in OA rats. The effect was achieved by the restoration of anabolism-catabolism balance through upregulation of OA-suppressed anabolic genes (*Col2* and *aggrecan*) and downregulation of OA-activated catabolic genes (*Col10*, *Mmp13*, *Adamts5*, and *Adamts9*) in chondrocytes. Its molecular mechanism was associated

with inhibition of NF- κ B signaling and blockage of c-Jun signaling in the TNF signaling pathway. This study provides certain knowledge of anti-OA effect and mechanism of PL, placing it as promising and alternative therapeutic option for OA therapy in the future.

MATERIALS AND METHODS

Chemicals and reagents

IMDM (Iscove's modified Dulbecco's medium) and trypsin (0.25%) were purchased from Thermo Fisher Scientific (MA, USA). FBS (fetal bovine serum) was purchased from CellMax (Beijing, China). MTT (3-(4,5-Dimethylthiazol-2-yl)-2,5-diphenyltetrazolium bromide) and DMSO (dimethyl sulfoxide) were purchased from Sigma-Aldrich (Taufkirchen, Germany). MIA was purchased from Sigma-Aldrich. The cell cycle kit was obtained from BD Biosciences (San Jose, CA, USA). Real time PCR (polymerase chain reaction) kit and TRIzol reagent were purchased from TaKaRa Biotechnology Co. Ltd. (Dalian, China). All primary antibodies were purchased from Cell Signaling Technology Inc. (Danvers, MA, USA). All ELISA kits were purchased from Multi Sciences (Lianke) Biotech Co., Ltd (Hangzhou, China).

Platelet concentrate preparation and PL extraction

Platelet lysate (PL) was obtained by lysing platelet concentrates of rat plasma according to the acknowledged method (2-step centrifugation procedure) with modifications [59]. Briefly, anti-coagulant whole blood (3% v/v sodium citrate) was treated by sequential rounds of centrifugation at 4 °C (10 min at $210 \times g$ and 5 min for $210 \times g$), with the non-erythrocyte volume collected subsequently to each round. The collected buffy coat was washed three times with PBS and concentrated through supernatant removal to obtain platelet concentrates. The final platelet number was measured by Mindray BC-3000plus blood cell analyzer (Shenzhen, China) and standardized to 1×10^8 platelets/ml. The platelet concentrate was lysed by repeating a freeze-thaw (-80°C to 37°C) three times, followed by centrifugation at $2,000 \times g$ for 10 min to remove remaining platelet fragments. The obtained supernatant containing bioactive growth factors (PL) was divided into aliquots and stored at -80°C before use.

Immunophenotypic analysis and enzyme-linked immunosorbent assay (ELISA)

The expression of platelet surface marker in platelet concentrates was assessed by flow cytometry analysis.

Before PL extraction, the platelet concentrates were suspended and incubated with the fluorochrome-conjugated antibody (anti-CD61-PE) against rat antigen for 1 h in the dark at RT. After incubation, PL was washed with PBS three times and re-suspended in PBS for flow cytometry analysis (BD FACSCalibur, BD Biosciences, CA, USA) in triplicates. Fluorescent signal intensity was recorded and analyzed by CellQuest software. After PL extraction, the concentrations of epidermal growth factor (EGF), insulin-like growth factor (IGF-1), platelet-derived growth factor (PDGF), transforming growth factor β (TGF- β), and vascular endothelial growth factor (VEGF) of PL were measured in triplicate using commercially available ELISA kits (Lianke Biotech Co., Hangzhou, China), in accordance with each manufacturer's instructions. The absorbance was measured using a microplate reader (Bio-Rad Laboratories, Inc., Hercules, CA, USA).

Animal and animal experiments

Male Sprague Dawley (SD) rats (Grade SPF II) with body weight of 200 ± 20 g were provided by Shanghai Super B&K Laboratory Animal Co. Ltd. (Certificate number: SCXK (Shanghai) 2013-0016). All rats were housed in cages under pathogen-free condition with 12 h light/dark cycle and provided with food and water ad libitum. The animal experiments were in accordance with the China legislation on the use and care of laboratory animals and approved by the Medical Norms and Ethics Committee of Zhejiang Chinese Medical University.

Fifty rats were equally and randomly divided into five groups: NC group as normal control group, model group as arthritis model group, PL-L as low dose of PL (10^5 platelet-derived PL) treated model group, PL-M as middle dose of PL (10^6 platelet-derived PL) treated model group, and PL-H as high dose of PL (10^7 platelet-derived PL) treated model group. The NC group was treated with 50 μ l of saline by intra-articular injection. The model group and all PL groups were treated with 50 μ l of MIA (30 mg/ml) by intra-articular injection for modeling of arthritis. After seven days, PL-L, PL-M, and PL-H groups were treated with 50 μ l of 10^5 platelet-derived PL, 10^6 platelet-derived PL, and 10^7 platelet-derived PL, respectively, by weekly intra-articular injection. Meanwhile, NC group was treated with 50 μ l of saline in a same route. After the treatments for four weeks, mechanical withdrawal threshold (MWT), thermal withdrawal latency (TWL), spontaneous activity, and treadmill gait analyses were measured. At the end of the experiment, all rats were euthanized by over anesthesia. Immediately, articular samples were taken from their knee joints for histopathological observation and immunohistochemical analysis.

Pain behavior and gait patterns analyses

The MWT, TWL, and spontaneous activity were measured as previously described [60]. Briefly, each rat was placed in a wire-mesh based cage for 30 min-acclimatization, followed by needling at its plantar surface of hind paws for three times. The needle pressure (g) which caused paw withdrawal was recorded as MWT. A focused beam of radiant heat was irradiated to the rat plantar surface of hind paws for three times, and the time length (s) before the heat-caused paw withdrawal was recorded as TWL. Each rat was placed in a dark box equipped with a monitor system for recording its activity, and the activity times within 10 min was recorded as the spontaneous activity parameter. The gait patterns of each rat, including paw area (cm²), stride length (cm), and body length (cm), were measured using the DigiGait System and the data captured by a video recorder (DigiGait Imaging System, Mouse Specifics, Boston, MA, USA). Total paw area (cm²), average stride length (cm) and Unite stride length were calculated.

Histopathological observation and immunohistochemical analysis

Each articular sample was fixed with formalin (10%) for 24 h and decalcified with EDTA (10%) in PBS for eight weeks. Then each sample was embedded in paraffin and sectioned into 2-3 μ m, followed by staining with HE (hematoxylin and eosin), SO (safranin-O), or ABH (alcian blue/hematoxylin). The stained sections were observed under microscopy and statistically graded on a scale of 0–13 by double-blind observation, according to the Mankin's scoring and OARSI scoring systems [61, 62]. Unstained replicates of the sections were incubated overnight at 4 °C with 100 μ l PBS-diluted (1:100) primary antibodies against rat Col2 (rabbit anti-Col2 monoclonal antibody) and rat matrix metalloproteinase 13 (mouse anti-Mmp13 monoclonal antibody). After PBS wash, the sections were incubated with Horseradish peroxidase (HRP) conjuncted secondary antibodies (PV-9001 for Col2 and PV-9002 for MMP13) (ZSGQ-BIO, Beijing, China) for 20 min at room temperature, followed by colorimetric detection using 3,3'-diaminobenzidine (DAB) substrate chromogen for 8 min. The immunoreactivity of Col2 and MMP13 were semiquantified by using Image-Pro Plus (IPP) 6.0 software (Media Cybernetics, Bethesda, MD, USA) under a light microscope (NIKON 80i, Tokyo, Japan).

Primary chondrocytes

Primary chondrocytes were obtained from allogeneic male SD rat donors as previously described [63].

Table 1. Primer sequences of target genes

Gene	Forward primer	Reverse primer
<i>β-actin</i>	5'-CCC GCGAGTACAACCTTCT-3'	5'-CGTCATCCATGGCGAACT-3'
<i>Col2</i>	5'-CTCAAGTCGCTGAACAACCA-3'	5'-GTCTCCGCTCTTCCACTCTG-3'
<i>Col10</i>	5'-GATCATGGAGCTCACGGAAAA-3'	5'-CCGTTTCGATTCCGCATTG-3'
<i>Mmp13</i>	5'-CTATGGTCCAGGAGATGAAGAC-3'	5'-GTGCAGACGCCAGAAGAATCT-3'
<i>Adamts5</i>	5'-TGGAGTGTGTGGAGGGGATA-3'	5'-CGGACTTTTATGTGGGTTGC-3'
<i>Adamts9</i>	5'-TACAGGCAAAGGCTGGTCTC-3'	5'-CTCAGGTAGCAGGGATGGAC-3'
<i>Aggrecan</i>	5'-GCAGACATTGATGAGTGCCTC-3'	5'-CTCACACAGGTCCCCTCTGT-3'

Briefly, articular cartilage tissues from four rat donors were harvested and sliced into small pieces. The pieces were digested with 0.25% trypsin for 40 min at 37°C and then with 0.1% Col2 for 4 h at 37°C. The isolated cells were filtered through a cell strainer (70 μm) and collected. The cells were identified as chondrocytes by morphology, toluidine blue staining and Col2 immunocytochemical staining. IMDM medium containing 10% FBS was used to culture the chondrocytes.

Cell viability assay

The cell viability of chondrocytes was evaluated by MTT assay, as previously described [60]. Briefly, the chondrocytes were seeded on 96-well plates for 24 h and treated with PLs derived from 10³, 10⁴, 10⁵, 10⁶, 10⁷, and 10⁸ platelets for another 24 h and 48 h. MTT solution was added to each well and incubated for 4 h. Subsequently, DMSO was added into each well to dissolve the formazan crystals. The optical density (OD) value was measured at 490 nm by a Bio-Rad microplate reader (Hercules, CA, USA). Proliferative rate (%) = (PL-treated OD/untreated OD) × 100.

Real time PCR (qPCR) assay

The primary chondrocytes were divided into three groups as follows: NC group was the normal control cultured for 30 h with no treatment; TNF-α group was the model group pre-treated with TNF-α (10 ng/ml) for 6 h and then cultured for 24 h with no further treatment; and TNF-α+PL group was the treatment group pre-treated with TNF-α (10 ng/ml) for 6 h and then treated with PL (derived from 10⁷ platelets) for 24 h. Total RNA was extracted with TRIzol reagent and quality controlled by NanoDrop2000 spectrophotometer (Thermo Scientific, USA) and agarose gel electrophoresis. The quality of all RNA samples was verified with good purity and integrity before use. Then, the reverse transcription was conducted to produce cDNA. As previously applied, the final qPCR reaction system was 20 μl, comprising 10 μl SYBR® Premix Ex Taq II (Tli RnaseH Plus), 0.4 μl PCR Forward Primer, 0.4 μl PCR Reverse Primer, 1 μl template cDNA and 8.2 μl ddH₂O, and the qPCR reaction conditions were

as follows: 95°C for 5 min for initial denaturation, followed by 40 cycles of denaturation at 95°C for 10 sec, annealing and extension at 60°C for 30 sec [60]. The qPCR assay was performed on an ABI QuantStudio™ 7 Flex Real-Time PCR System (Applied Biosystems; Thermo Scientific, USA). β-Actin was used as the reference gene and 2^{-ΔΔCT} method was applied to measure the relative mRNA expression (Table 1).

Western blot (WB) analysis

The chondrocytes were grouped and treated in accordance with qPCR assay procedure. As previously described, the total proteins were extracted by using lysis buffer (50 mM Tris-HCl, pH 7.4, 150 mM NaCl, 1 mM EDTA, 1% Triton and 0.1% SDS) with proteinase inhibitor cocktail (Bimake, Houston, TX, USA) for 30 min on ice [64]. Proteins were separated by SDS-PAGE (6-12%) and transferred onto a nitrocellulose membrane (Sartorius Stedim, Göttingen, Germany). The membrane was blocked with 5% non-fat milk for 2 h, followed by overnight incubation at 4°C with primary antibodies including actin, Col10, Mmp13, total NF-κB p65, phosphor-NF-κB p65, phosphor-IKKα/β, phosphor-c-Jun, poly (ADP-ribose) polymerase (PARP), and cleaved-PARP. Following incubation with peroxidase-conjugated goat anti-rabbit/mouse IgG at room temperature for 2 h, proteins were visualized using Western Lightning® Plus ECL (Perkin Elmer, Inc., Waltham, MA, USA), detected using X-ray film (Kodak, Tokyo, Japan) and scanned [64].

Statistical analysis

Data were expressed as the mean ± standard deviation (SD). Data from different groups were compared using one-way ANOVA followed by Fisher's least significant difference (LSD) comparison. A *p*-value < 0.05 was considered to indicate a significant difference and *p*-value < 0.01 considered to indicate a very significant difference. The Mankin's score and OARSI score were assessed by three independent observers in a blind manner. All analyses were performed using an updated version of DPS software [65].

Abbreviations

ABH: alcian blue hematoxylin; AP-1: activator protein 1; Col2: collagen II; ECM: extracellular matrix; EGF: epidermal growth factor; HE: hematoxylin-eosin; IGF: insulin-like growth factor; IKK: inhibitory κ B kinase; IL-1: interleukin-1; IMDM: Iscove's modified Dulbecco's medium; JNK: c-Jun N-terminal kinase; KOOS: Knee Osteoarthritis and Disability Outcome Score; LSD: least significant difference; MIA: monoiodoacetate; MMP: matrix metalloproteinase; MWT: mechanical withdrawal threshold; NC: normal control; NF- κ B: nuclear factor κ B; OA: osteoarthritis; OARSI: Osteoarthritis Research International; PARP: poly (ADP-ribose) polymerase; PBS: phosphate buffered saline; PDGF: platelet derived growth factors; PL: platelet lysate; PRP: platelet rich plasma; SD: standard deviation; sGAG: sulfated glycosaminoglycan; SO: safranin-O; SD rats: Sprague Dawley rats; TGF- β : transforming growth factor- β ; TNF- α : tumor necrosis factor α ; TWL: thermal withdrawal latency; VEGF: vascular endothelial growth factor.

AUTHOR CONTRIBUTIONS

Li Yan and Li Zhou performed the main experiments; Danting Xie contributed to the PL preparation and quality control; Letian Shan designed the experiments, wrote the manuscript and revised the manuscript; Qiang Yuan improved the experimental design and methodology; Fangming Chen contributed to the revision. Wenxi Du and Peijian Tong provided the funding support to this study; Thomas Efferth improved the design, draft, revision and language editing of this manuscript. All authors agreed the submission of this manuscript, and agreed to be accountable for all aspects of this work.

ACKNOWLEDGMENTS

This study was funded by the Zhejiang Provincial Natural Science Foundation of China (Grant No: LY16H270011, LY16H060005, and LY17H270016), the Major Science and Technology Special Project of Zhejiang Province (Grant No: 2014C03035), the National Natural Science Foundation of China (Grant No: 81774331, 81873049, and 81673997), and the Zhejiang Provincial Science and Technology Project of Traditional Chinese Medicine of China (Grant No: 2013ZQ007 and 2016ZZ011).

CONFLICTS OF INTEREST

No conflicts of interest exists in this manuscript.

REFERENCES

1. Zhu Y, Yuan M, Meng HY, Wang AY, Guo QY, Wang Y, Peng J. Basic science and clinical application of platelet-rich plasma for cartilage defects and osteoarthritis: a review. *Osteoarthritis Cartilage*. 2013; 21:1627–37. <https://doi.org/10.1016/j.joca.2013.07.017> PMID:23933379
2. Wittenauer R, Smith L, Aden K. Priority Medicines for Europe and the World 2013 Update. Background Paper 6.12 Osteoarthritis. WHO Essential Medicines and Health Products Information Portal. 2013. <http://apps.who.int/medicinedocs/en/m/abstract/Js20259en/>
3. Zhang Y, Jordan JM. Epidemiology of osteoarthritis. *Clin Geriatr Med*. 2010; 26:355–69. <https://doi.org/10.1016/j.cger.2010.03.001> PMID:20699159
4. Flanigan DC, Harris JD, Trinh TQ, Siston RA, Brophy RH. Prevalence of chondral defects in athletes' knees: a systematic review. *Med Sci Sports Exerc*. 2010; 42:1795–801. <https://doi.org/10.1249/MSS.0b013e3181d9eea0> PMID:20216470
5. Altman RD, Devji T, Bhandari M, Fierlinger A, Niazi F, Christensen R. Clinical benefit of intra-articular saline as a comparator in clinical trials of knee osteoarthritis treatments: A systematic review and meta-analysis of randomized trials. *Semin Arthritis Rheum*. 2016; 46:151–59. <https://doi.org/10.1016/j.semarthrit.2016.04.003> PMID:27238876
6. He WW, Kuang MJ, Zhao J, Sun L, Lu B, Wang Y, Ma JX, Ma XL. Efficacy and safety of intraarticular hyaluronic acid and corticosteroid for knee osteoarthritis: A meta-analysis. *Int J Surg*. 2017; 39:95–103. <https://doi.org/10.1016/j.ijsu.2017.01.087> PMID:28137554
7. Brown GA. AAOS clinical practice guideline: treatment of osteoarthritis of the knee: evidence-based guideline, 2nd edition. *J Am Acad Orthop Surg*. 2013; 21:577–79. <https://doi.org/10.5435/JAAOS-21-09-577> PMID:23996989
8. Meheux CJ, McCulloch PC, Lintner DM, Varner KE, Harris JD. Efficacy of Intra-articular Platelet-Rich Plasma Injections in Knee Osteoarthritis: A Systematic Review. *Arthroscopy*. 2016; 32:495–505. <https://doi.org/10.1016/j.arthro.2015.08.005> PMID:26432430

9. Eastment CT, Sirbasku DA. Human platelet lysate contains growth factor activities for established cell lines derived from various tissues of several species. *In Vitro*. 1980; 16:694–705. <https://doi.org/10.1007/BF02619199> PMID:7419237
10. Hara Y, Steiner M, Baldini MG. Platelets as a source of growth-promoting factor(s) for tumor cells. *Cancer Res*. 1980; 40:1212–16. PMID:7357550
11. Choi YC, Morris GM, Sokoloff L. Effect of platelet lysate on growth and sulfated glycosaminoglycan synthesis in articular chondrocyte cultures. *Arthritis Rheum*. 1980; 23:220–24. <https://doi.org/10.1002/art.1780230213> PMID:7362669
12. Blair P, Flaumenhaft R. Platelet alpha-granules: basic biology and clinical correlates. *Blood Rev*. 2009; 23:177–89. <https://doi.org/10.1016/j.blre.2009.04.001> PMID:19450911
13. Golebiewska EM, Poole AW. Platelet secretion: from haemostasis to wound healing and beyond. *Blood Rev*. 2015; 29:153–62. <https://doi.org/10.1016/j.blre.2014.10.003> PMID:25468720
14. Nurden AT, Nurden P, Sanchez M, Andia I, Anitua E. Platelets and wound healing. *Front Biosci*. 2008; 13:3532–48. <http://dx.doi.org/10.2741/2947> PMID:18508453
15. Fortier LA, Barker JU, Strauss EJ, McCarrel TM, Cole BJ. The role of growth factors in cartilage repair. *Clin Orthop Relat Res*. 2011; 469:2706–15. <https://doi.org/10.1007/s11999-011-1857-3> PMID:21403984
16. Montaseri A, Busch F, Mobasher A, Buhrmann C, Aldinger C, Rad JS, Shakibaei M. IGF-1 and PDGF-bb suppress IL-1 β -induced cartilage degradation through down-regulation of NF- κ B signaling: involvement of Src/PI-3K/AKT pathway. *PLoS One*. 2011; 6:e28663. <https://doi.org/10.1371/journal.pone.0028663> PMID:22194879
17. Asanbaeva A, Masuda K, Thonar EJ, Klisch SM, Sah RL. Regulation of immature cartilage growth by IGF-I, TGF-beta1, BMP-7, and PDGF-AB: role of metabolic balance between fixed charge and collagen network. *Biomech Model Mechanobiol*. 2008; 7:263–76. <https://doi.org/10.1007/s10237-007-0096-8> PMID:17762943
18. Makower AM, Wroblewski J, Pawlowski A. Effects of IGF-I, rGH, FGF, EGF and NCS on DNA-synthesis, cell proliferation and morphology of chondrocytes isolated from rat rib growth cartilage. *Cell Biol Int Rep*. 1989; 13:259–70. PMID:2706688
19. Tyrnenopoulou P, Diakakis N, Karayannopoulou M, Savvas I, Koliakos G. Evaluation of intra-articular injection of autologous platelet lysate (PL) in horses with osteoarthritis of the distal interphalangeal joint. *Vet Q*. 2016; 36:56–62. <https://doi.org/10.1080/01652176.2016.1141257> PMID:26828234
20. Al-Ajlouni J, Awidi A, Samara O, Al-Najar M, Tarwanah E, Saleh M, Awidi M, Hassan FA, Samih M, Bener A, Dweik M. Safety and efficacy of autologous intra-articular platelet lysates in early and intermediate knee osteoarthritis in humans: a prospective open-label study. *Clin J Sport Med*. 2015; 25:524–28. <https://doi.org/10.1097/JSM.000000000000166> PMID:25387167
21. Kawarai Y, Orita S, Nakamura J, Miyamoto S, Suzuki M, Inage K, Hagiwara S, Suzuki T, Nakajima T, Akazawa T, Ohtori S. Changes in proinflammatory cytokines, neuropeptides, and microglia in an animal model of monosodium iodoacetate-induced hip osteoarthritis. *J Orthop Res*. 2018; 36:2978–86. <https://doi.org/10.1002/jor.24065> PMID:29888808
22. Takatori N, Sato M, Toyoda E, Takahashi T, Okada E, Maehara M, Watanabe M. Cartilage repair and inhibition of the progression of cartilage degeneration after transplantation of allogeneic chondrocyte sheets in a nontraumatic early arthritis model. *Regen Ther*. 2018; 9:24–31. <https://doi.org/10.1016/j.reth.2018.07.003> PMID:30525072
23. Lampropoulou-Adamidou K, Lelovas P, Karadimas EV, Liakou C, Triantafillopoulos IK, Dontas I, Papaioannou NA. Useful animal models for the research of osteoarthritis. *Eur J Orthop Surg Traumatol*. 2014; 24:263–71. <https://doi.org/10.1007/s00590-013-1205-2> PMID:23508348
24. Morais SV, Czczko NG, Malafaia O, Ribas JM, Garcia JB, Miguel MT, Zini C, Massignan AG. Osteoarthritis model induced by intra-articular monosodium iodoacetate in rats knee. *Acta Cir Bras*. 2016; 31:765–73. <https://doi.org/10.1590/s0102-865020160110000010> PMID:27982265
25. Mohan G, Perilli E, Kuliwaba JS, Humphries JM, Parkinson IH, Fazzalari NL. Application of in vivo micro-computed tomography in the temporal characterisation of subchondral bone architecture in a rat model of low-dose monosodium iodoacetate-induced osteoarthritis. *Arthritis Res Ther*. 2011; 13:R210. <https://doi.org/10.1186/ar3543> PMID:22185204
26. Udo M, Muneta T, Tsuji K, Ozeki N, Nakagawa Y, Ohara T, Saito R, Yanagisawa K, Koga H, Sekiya I. Monoiodoacetic acid induces arthritis and synovitis in

- rats in a dose- and time-dependent manner: proposed model-specific scoring systems. *Osteoarthritis Cartilage*. 2016; 24:1284–91. <https://doi.org/10.1016/j.joca.2016.02.005> PMID:26915639
27. Barve RA, Minnerly JC, Weiss DJ, Meyer DM, Aguiar DJ, Sullivan PM, Weinrich SL, Head RD. Transcriptional profiling and pathway analysis of monosodium iodoacetate-induced experimental osteoarthritis in rats: relevance to human disease. *Osteoarthritis Cartilage*. 2007; 15:1190–98. <https://doi.org/10.1016/j.joca.2007.03.014> PMID:17500014
28. Charlier E, Relic B, Deroyer C, Malaise O, Neuville S, Collée J, Malaise MG, De Seny D. Insights on molecular mechanisms of chondrocytes death in osteoarthritis. *Int J Mol Sci*. 2016; 17:17. <https://doi.org/10.3390/ijms17122146> PMID:27999417
29. Archer CW, Francis-West P. The chondrocyte. *Int J Biochem Cell Biol*. 2003; 35:401–04. [https://doi.org/10.1016/S1357-2725\(02\)00301-1](https://doi.org/10.1016/S1357-2725(02)00301-1) PMID:12565700
30. Larsson S, Englund M, Struglics A, Lohmander LS. Interleukin-6 and tumor necrosis factor alpha in synovial fluid are associated with progression of radiographic knee osteoarthritis in subjects with previous meniscectomy. *Osteoarthritis Cartilage*. 2015; 23:1906–14. <https://doi.org/10.1016/j.joca.2015.05.035> PMID:26521736
31. Greene MA, Loeser RF. Aging-related inflammation in osteoarthritis. *Osteoarthritis Cartilage*. 2015; 23:1966–71. <https://doi.org/10.1016/j.joca.2015.01.008> PMID:26521742
32. Penninx BW, Abbas H, Ambrosius W, Nicklas BJ, Davis C, Messier SP, Pahor M. Inflammatory markers and physical function among older adults with knee osteoarthritis. *J Rheumatol*. 2004; 31:2027–31. PMID:15468370
33. Forsyth CB, Cole A, Murphy G, Bienias JL, Im HJ, Loeser RF Jr. Increased matrix metalloproteinase-13 production with aging by human articular chondrocytes in response to catabolic stimuli. *J Gerontol A Biol Sci Med Sci*. 2005; 60:1118–24. <https://doi.org/10.1093/gerona/60.9.1118> PMID:16183949
34. Goldring MB, Otero M, Plumb DA, Dragomir C, Favero M, El Hachem K, Hashimoto K, Roach HI, Olivotto E, Borzi RM, Marcu KB. Roles of inflammatory and anabolic cytokines in cartilage metabolism: signals and multiple effectors converge upon MMP-13 regulation in osteoarthritis. *Eur Cell Mater*. 2011; 21:202–20. <https://doi.org/10.22203/eCM.v021a16> PMID:21351054
35. Liacini A, Sylvester J, Li WQ, Huang W, Dehnade F, Ahmad M, Zafarullah M. Induction of matrix metalloproteinase-13 gene expression by TNF-alpha is mediated by MAP kinases, AP-1, and NF-kappaB transcription factors in articular chondrocytes. *Exp Cell Res*. 2003; 288:208–17. [https://doi.org/10.1016/S0014-4827\(03\)00180-0](https://doi.org/10.1016/S0014-4827(03)00180-0) PMID:12878172
36. Caterson B, Flannery CR, Hughes CE, Little CB. Mechanisms involved in cartilage proteoglycan catabolism. *Matrix Biol*. 2000; 19:333–44. [https://doi.org/10.1016/S0945-053X\(00\)00078-0](https://doi.org/10.1016/S0945-053X(00)00078-0) PMID:10963994
37. Shiomi T, Lemaître V, D’Armiento J, Okada Y. Matrix metalloproteinases, a disintegrin and metalloproteinases, and a disintegrin and metalloproteinases with thrombospondin motifs in non-neoplastic diseases. *Pathol Int*. 2010; 60:477–96. <https://doi.org/10.1111/j.1440-1827.2010.02547.x> PMID:20594269
38. Song RH, Tortorella MD, Malfait AM, Alston JT, Yang Z, Arner EC, Griggs DW. Aggrecan degradation in human articular cartilage explants is mediated by both ADAMTS-4 and ADAMTS-5. *Arthritis Rheum*. 2007; 56:575–85. <https://doi.org/10.1002/art.22334> PMID:17265492
39. Glasson SS, Askew R, Sheppard B, Carito B, Blanchet T, Ma HL, Flannery CR, Peluso D, Kanki K, Yang Z, Majumdar MK, Morris EA. Deletion of active ADAMTS5 prevents cartilage degradation in a murine model of osteoarthritis. *Nature*. 2005; 434:644–48. <https://doi.org/10.1038/nature03369> PMID:15800624
40. Wang M, Sampson ER, Jin H, Li J, Ke QH, Im HJ, Chen D. MMP13 is a critical target gene during the progression of osteoarthritis. *Arthritis Res Ther*. 2013; 15:R5. <https://doi.org/10.1186/ar4133> PMID:23298463
41. Walker GD, Fischer M, Gannon J, Thompson RC Jr, Oegema TR Jr. Expression of type-X collagen in osteoarthritis. *J Orthop Res*. 1995; 13:4–12. <https://doi.org/10.1002/jor.1100130104> PMID:7853102
42. He Y, Siebuhr AS, Brandt-Hansen NU, Wang J, Su D, Zheng Q, Simonsen O, Petersen KK, Arendt-Nielsen L, Eskehave T, Hoeck HC, Karsdal MA, Bay-Jensen AC. Type X collagen levels are elevated in serum from human osteoarthritis patients and associated with

- biomarkers of cartilage degradation and inflammation. *BMC Musculoskelet Disord*. 2014; 15:309. <https://doi.org/10.1186/1471-2474-15-309> PMID:25245039
43. Roman-Blas JA, Jimenez SA. NF-kappaB as a potential therapeutic target in osteoarthritis and rheumatoid arthritis. *Osteoarthritis Cartilage*. 2006; 14:839–48. <https://doi.org/10.1016/j.joca.2006.04.008> PMID:16730463
 44. Kobayashi H, Hirata M, Saito T, Itoh S, Chung UI, Kawaguchi H. Transcriptional induction of ADAMTS5 protein by nuclear factor- κ B (NF- κ B) family member RelA/p65 in chondrocytes during osteoarthritis development. *J Biol Chem*. 2013; 288:28620–29. <https://doi.org/10.1074/jbc.M113.452169> PMID:23963448
 45. Tao R, Xu X, Sun C, Wang Y, Wang S, Liu Z, Zhai L, Cheng H, Xiao M, Zhang D. KPNA2 interacts with P65 to modulate catabolic events in osteoarthritis. *Exp Mol Pathol*. 2015; 99:245–52. <https://doi.org/10.1016/j.yexmp.2015.07.007> PMID:26209501
 46. Lianxu C, Hongti J, Changlong Y. NF-kappaBp65-specific siRNA inhibits expression of genes of COX-2, NOS-2 and MMP-9 in rat IL-1beta-induced and TNF-alpha-induced chondrocytes. *Osteoarthritis Cartilage*. 2006; 14:367–76. <https://doi.org/10.1016/j.joca.2005.10.009> PMID:16376111
 47. Chen LW, Liu FC, Hung LF, Huang CY, Lien SB, Lin LC, Lai JH, Ho LJ. Chondroprotective effects and mechanisms of dextromethorphan: repurposing antitussive medication for osteoarthritis treatment. *Int J Mol Sci*. 2018; 19:19. <https://doi.org/10.3390/ijms19030825> PMID:29534535
 48. Dhanasekaran DN, Reddy EP. JNK signaling in apoptosis. *Oncogene*. 2008; 27:6245–51. <https://doi.org/10.1038/onc.2008.301> PMID:18931691
 49. Shi J, Zhang C, Yi Z, Lan C. Explore the variation of MMP3, JNK, p38 MAPKs, and autophagy at the early stage of osteoarthritis. *IUBMB Life*. 2016; 68:293–302. <https://doi.org/10.1002/iub.1482> PMID:26873249
 50. Chen Q, Gao Y, Kao X, Chen J, Xue W, Xiong Y, Wang Z. SNP-induced apoptosis may be mediated with caspase inhibitor by JNK signaling pathways in rabbit articular chondrocytes. *J Toxicol Sci*. 2012; 37:157–67. <https://doi.org/10.2131/jts.37.157> PMID:22293420
 51. Ho LJ, Hung LF, Liu FC, Hou TY, Lin LC, Huang CY, Lai JH. Ginkgo biloba extract individually inhibits JNK activation and induces c-Jun degradation in human chondrocytes: potential therapeutics for osteoarthritis. *PLoS One*. 2013; 8:e82033. <https://doi.org/10.1371/journal.pone.0082033> PMID:24349175
 52. Andia I, Sánchez M, Maffulli N. Joint pathology and platelet-rich plasma therapies. *Expert Opin Biol Ther*. 2012; 12:7–22. <https://doi.org/10.1517/14712598.2012.632765> PMID:22171664
 53. Xie X, Zhang C, Tuan RS. Biology of platelet-rich plasma and its clinical application in cartilage repair. *Arthritis Res Ther*. 2014; 16:204. <https://doi.org/10.1186/ar4493> PMID:25164150
 54. Maffulli N, Del Buono A. Platelet plasma rich products in musculoskeletal medicine: any evidence? *Surgeon*. 2012; 10:148–50. <https://doi.org/10.1016/j.surge.2011.03.004> PMID:22525416
 55. Altaie A, Owston H, Jones E. Use of platelet lysate for bone regeneration - are we ready for clinical translation? *World J Stem Cells*. 2016; 8:47–55. <https://doi.org/10.4252/wjsc.v8.i2.47> PMID:26981170
 56. Klatt-Schulz F, Schmidt T, Uckert M, Scheffler S, Kalus U, Rojewski M, Schrenzenmeier H, Pruss A, Wildemann B. Comparative analysis of different platelet lysates and platelet rich preparations to stimulate tendon cell biology: an in vitro study. *Int J Mol Sci*. 2018; 19:19. <https://doi.org/10.3390/ijms19010212> PMID:29320421
 57. Sykes JG, Kuiper JH, Richardson JB, Roberts S, Wright KT, Kuiper NJ. Impact of human platelet lysate on the expansion and chondrogenic capacity of cultured human chondrocytes for cartilage cell therapy. *Eur Cell Mater*. 2018; 35:255–67. <https://doi.org/10.22203/eCM.v035a18> PMID:29714398
 58. Hildner F, Eder MJ, Hofer K, Aberl J, Redl H, van Griensven M, Gabriel C, Peterbauer-Scherb A. Human platelet lysate successfully promotes proliferation and subsequent chondrogenic differentiation of adipose-derived stem cells: a comparison with articular chondrocytes. *J Tissue Eng Regen Med*. 2015; 9:808–18. <https://doi.org/10.1002/term.1649> PMID:23303715
 59. Nguyen VT, Cancedda R, Descalzi F. Platelet lysate activates quiescent cell proliferation and reprogramming in human articular cartilage: involvement of hypoxia inducible factor 1. *J Tissue Eng Regen Med*. 2018; 12:e1691–703.

- <https://doi.org/10.1002/term.2595> PMID:29052350
60. Yan B, Zhou L, Wang C, Wang R, Yan L, Yu L, Liu F, Du W, Yu G, Yuan Q, Tong P, Shan L, Efferth T. Intra-articular injection of fructus ligustri lucidi extract attenuates pain behavior and cartilage degeneration in mono-iodoacetate induced osteoarthritic rats. *Front Pharmacol*. 2018; 9:1360. <https://doi.org/10.3389/fphar.2018.01360> PMID:30532708
61. Mankin HJ, Lippiello L. Biochemical and metabolic abnormalities in articular cartilage from osteoarthritic human hips. *J Bone Joint Surg Am*. 1970; 52:424–34. <https://doi.org/10.2106/00004623-197052030-00002> PMID:4246573
62. Glasson SS, Chambers MG, Van Den Berg WB, Little CB. The OARSI histopathology initiative - recommendations for histological assessments of osteoarthritis in the mouse. *Osteoarthritis Cartilage*. 2010 (Suppl 3); 18:S17–23. <https://doi.org/10.1016/j.joca.2010.05.025> PMID:20864019
63. Tong P, Xu S, Cao G, Jin W, Guo Y, Cheng Y, Jin H, Shan L, Xiao L. Chondroprotective activity of a detoxicated traditional Chinese medicine (FuZi) of *Aconitum carmichaeli* Debx against severe-stage osteoarthritis model induced by mono-iodoacetate. *J Ethnopharmacol*. 2014; 151:740–44. <https://doi.org/10.1016/j.jep.2013.11.048> PMID:24315981
64. Wang C, Yan L, Yan B, Zhou L, Sun W, Yu L, Liu F, Du W, Yu G, Hu Z, Yuan Q, Xiao L, Li H, et al. Agkistrodon ameliorates pain response and prevents cartilage degradation in monosodium iodoacetate-induced osteoarthritic rats by inhibiting chondrocyte hypertrophy and apoptosis. *J Ethnopharmacol*. 2019; 231:545–54. <https://doi.org/10.1016/j.jep.2018.12.004> PMID:30529425
65. Tang QY, Feng MG. DPS data processing system: experimental design, statistical analysis and data mining. China: Beijing Science Press; 2007.